Iranian Journal of Analytical Chemistry
Volume 4, Issue 2, September 2017 (22-32)

مجله ایرانی شیمی تجزیه
دوره ۴، شماره ۲، مهر ماه ۱۳۹۶ (۳۲-۲۲)

جذب سطحی یون‌های فلزی مس، روی و سرب از نمونه‌های آبی با استفاده از نانوذرات مغناطیسی Fe_3O_4 اصلاح‌شده با آلیزارین قرمز اس

صدیقه کامران
بخش شیمی، دانشگاه پیام نور، صندوق پستی ۳۶۹۷-۱۹۳۹۵، تهران، ایران
تاریخ دریافت: ۲۷ اردیبهشت ۱۳۹٦ تاریخ پذیرش: ۲۳ مرداد ۱۳۹٦

Adsorption of Copper, Zinc and Lead Metal Ions from Aqueous Samples Using Fe_3O_4 Magnetic Nanoparticles Modified with Alizarin Red S

Sedigheh Kamran
Department of Chemistry, Payame Noor University, P.O.BOX 19395-3697 Tehran, Iran
Received: 17 May 2017 **Accepted:** 14 August 2017

چکیده

نانوذرات مغناطیسی Fe_3O_4 اصلاح‌شده با آلیزارین قرمز اس برای حذف چند یون فلزی از محلول آبی استفاده شد. اندازه و ریخت‌شناسی نانوذرات بوسیله تکنیک‌های TEM، XRD وFTIR تعیین گردید. مطالعات جذب سطحی یون‌های مورد نظر در سیستم ثابت انجام گرفت. جذب سطحی برسطح نانوذرات (ARS-Fe_3O_4) تحت تأثیر چندین پارامتر تجزیه‌ای مانند: pH اولیه، غلظت یون‌های فلزی، مقدار جاذب، زمان تماس و درجه حرارت می‌باشد. نتایج آزمایشات نشان داد که نانوذرات (ARS-Fe3O4) بطور کمی یون‌های مورد نظر را حذف می‌نماید. ماکزیمم ظرفیت جذب سطحی نانوذرات برطبق مدل لانگمیر ۵۰/۰، ۲۲/۷ و ۲۱/۷ میلی‌گرم هریک از یون‌های Zn^{2+}، Cu^{2}+ و Pb^{2}+ بر گرم نانوذرات می‌باشد. محاسبات همدما نشان داد که داده‌های تعادلی با مدل لانگمیر نسبت به سایر مدل‌ها تطابق بهتری دارد. داده‌های سینتیکی جذب سطحی یون‌های Zn^{2+} ، Cu^{2}+ و Pb^{2}+ برروی جاذب تهیه‌شده با معادله سینتیکی شبه درجه دوم بهتر توصیف می‌شود. فرآیند جذب سطحی در مورد هر سه یون مورد مطالعه گرماگیر است و این یون‌های فلزی توسط ۲ میلی‌لیتر محلول اسید کلریدریک ۰/۱ مول بر لیتر از سطح جاذب واجذب می‌گردد.

واژه‌های کلیدی

نانوذرات مغناطیسی؛ آلیزارین قرمز اس؛ جذب سطحی؛ حذف یون‌های فلزی.

Abstract

Fe_3O_4 magnetic nanoparticles modified with alizarin red S (ARS-Fe_3O_4) were used for the removal of several metal ions from aqueous solution. The mean size and the surface morphology of the nanoparticles were characterized by TEM, XRD and FTIR techniques. Adsorption studies of mentioned metal ions were performed in batch system. The adsorption of metal ions onto ARS-Fe_3O_4 nanoparticles was affected by the several analytical parameters such as an initial pH, metal ions concentration, adsorbent amount, contact time and temperature. Experimental results indicated that ARS-Fe_3O_4 nanoparticles were quantitatively removed. The maximum adsorption capacities of ARS-Fe_3O_4 for the Langmuir model were 50.0, 22.7 and 21.7 mg of metal ions per gram of nanoparticle for Zn^{2+}, Cu^{2+} and Pb^{2+}, respectively. The isotherm evaluations revealed that the Langmuir model attained better fits to the equilibrium data than the othermodels. The kinetic data of adsorption of Zn^{2+}, Cu^{2+} and Pb^{2+} ions on the synthesized adsorbents were best described by pseudo-second-order equation. The adsorption processesfor three metal ions were endothermic. Metal ions were desorbed from nanoparticles by 2 mLHCl solution 0.1 mol L^{-1}.

Keywords
Magnetic Nanoparticle; Alizarin Red S; Adsorption; Removal of Metal Ions.

1. INTRODUCTION

The heavy metal ions are not only dangerous for aquatic organisms, but also cause toxic effects to landanimals including humans through food chain transfers. Heavy metal ions can specially bind toproteins, nucleic acids and small metabolites, in living organisms. The contaminated organic cellsare altered or missed their biological functions with losing thehomeostatic control of essential metals, resulting in fatal healthproblems. Therefore, it is necessary to eliminate such hazardousheavy metal ion in wastewater before

*Corresponding Author: kamran_ss5@yahoo.com &s.kamran@pnu.ac.ir

discharging it into theenvironment.Water contaminated by heavy metalionss had become much more serious with a rapid development of industries and competitive use of fresh water in many parts of worlds [1-4]. Waste waters from many industries such as metallurgical,tannery, chemical manufacturing, mining, battery manufacturingindustries, etc. contain one or more toxic heavy metal ions. It is necessaryto remove these ions from the waste waters before releasingthem into the environment. There has been increasing concern andmore stringent regulation standards pertaining to the discharge ofheavy metal ions into the aquatic environment [3-4]. Many technologies and methods for heavy metal ions removalfrom waste waters have been developed, such as ion-exchange, evaporation and concentration, chemical precipitation, reverse-osmosis, adsorption and electrodialysis.

Considering from economy and efficiency point of view, adsorption is regarded as one ofthe most promising and widely used methods.A number of materials, including activated carbon [5-6], fly ash [7-8], peat [9], sewage sludge ash [10], zeolites [11], biomaterials [12-13], recycled alum sludge [14], manganese oxides [15],peanut hulls [16], kaolinite [17] resins [18],alumina modified by surfactant [19], Octadecyl silica [20] and etc have been reported to be capable of adsorbing heavy metal ions from aqueous solutions. Nevertheless, these materialshave some inherent disadvantages such as low adsorption capacities or high costs, which place urgent needs for the development ofnew adsorbent materials aimed at protecting our water and ensuring widespread access to clean and affordable potable water [21]. Therefore, research fornew and more effective materials to be used as adsorbents is acontinuous effort for many researchers. Nanomaterials have large specific surface areas and thus a large fraction of active sites are available for appropriate chemical interaction [22]. Surface modification of magnetic nanoparticles can be accomplished by physical/chemical adsorption of organic compounds by four major techniques: organic vapor condensation, polymer coating, surfactant adsorption and direct silanation [23].

This paper focuses on the preparation of magnetic nanoparticles of Fe_3O_4 modified by alizarin red S (ARS-Fe_3O_4) and characterization by Thermal electron microscopy (TEM), Fourier transform infrared (FTIR) spectroscopy and X ray Diffraction (XRD). Removal of Zn^{2+}, Cu^{2+} and Pb^{2+} onto Fe_3O_4 modified alizarin red S was studied. The effects of different experimental conditions such as dosage of nanoparticle, concentrations of metal ions, pH of the aqueous sample and contact times, on removal of three metal ions were evaluated. Adsorption isotherms, kinetic of adsorption andthermody-namic parameters were characterized as well. To the best of our knowledge, adsorption of these metal ions onto Fe_3O_4 magenetic nanoparticles modified by ARS has not been reported.

2. EXPERIMENTAL

2.1. Apparatus

An atomic absorption spectrometer of GBC SCIENTIFIC EQUIPMENT model was used for determination of of Zn^{2+}, Cu^{2+} and Pb^{2+}. The following conditions were used: absorption line; Cu: 327.4 nm, Zn: 213.9 nm, Pb: 405.8 nm; slit width: 0.5 nm; and lamp currents: 4 mA. The follow rates of air and acetylene were set as recommended by the manufacturer. A double beam UV-visible Shimadzu spectrophotometer Model 1601 equipped with a 1-cm quartz cell was used for recording the visible spectra and absorbance measurements. The infrared spectra were recorded by KBr pellets using FT-IR spectrometer model PerkinElmer Spectrum RXI.The XRD measurements were performed on the XRD Bruker D8 Advance. A transmission electron microscope (Philips CM 10 TEM) was used for recording the TEM images. A Metrohm780 pH meter was used for monitoring the pH values. A water Ultrasonicator (Model CD-4800, China) was used to disperse the nanoparticles in solution and a super magnet Nd–Fe–B (1.47 T, 10×5×2 cm) was used. All measurements were performed at ambient temperature.

2.2. Chemicals and reagents

All chemicals and reagents were of analytical grades. Alizarin red S (scheme 1), sodium chloride, $FeCl_3.6H_2O$ (96 %w/w) and $FeSO_4.7H_2O$ (99.9 %w/w) were purchased from Merck (Darmstadt, Germmany). The stock solution of copper sulphate pentahydrate ($CuSO_4.5H_2O$), zinc nitrate hexahydrate ($Zn(NO_3)_2.6H_2O$) and lead nitrate ($Pb(NO_3)_2$) were prepared by dissolving an accurately weighed amount of the salts in deionized water. The experimental solutions were prepared by diluting the stock solution with distilled water when necessary. The pH adjustments were performed with HCl and NaOH solutions (0.01-1.0 mol L^{-1}).

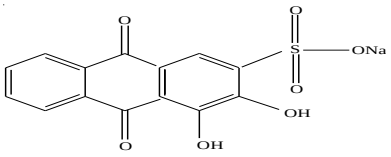

Scheme 1. Chemical Structure of alizarin red S.

2.3. Fabrication of ARS-modified magnetic nanoparticles

The nanoparticles of Fe_3O_4 were synthesized by mixing ferrous sulfate and ferric chloride in NaOH solution with constant stirring as recommended [24]. To obtain maximum yield for magnetic nanoparticles during co-precipitation process, the ideal molar ratio of Fe^{2+}/Fe^{3+} was about 0.5. The precipitates were heated at 80 °C for 30 minutes and were sonicated for 20 minutes, then washed three times with 50 mL distilled water solution.

Modification of Fe_3O_4 nanoparticles was carried out using alizarin red S at room temperature. In order to modify the nanoparticles, 20 mL of ARS solution (30 mg L^{-1}, pH 3.0) was added to about 0.025 g of damped nanoparticles in a beaker and the solution was stirred for 30 min by a glassy rod, followed by stiring using a magnetic stirrer. The modified magnetite nanoparticles (ARS-Fe_3O_4) were collected by applying a magnetic field with an intensity of 1.4 T. The ARS-Fe_3O_4 nanoparticles were washed three times with 50 mL distilled water. Nanoparticles and distilled water mixture was dispersed by ultrasonicator for 10 minutes at room temperature. Finally, the ARS-Fe_3O_4 nanoparticles were magnetically separated.

2.4. Adsorption equilibrium of metal ions

Adsorption of metal ions ontoARS-Fe_3O_4 nanoparticles from aqueous solutions was investigated batch-wise. The magnetic nanoparticles (0.025g) were incubated with 5 mL of the aqueous solutions of metal ions for 2-25 minutes (equilibrium time) in a beaker agitated magnetically at 150 rpm. After mixing, magnet was removed and washed with distilled water. Then the adsorbed metal ions on the surface of ARS-Fe_3O_4 nanoparticles was magnetically separated and the mother solution was analyzed for the residual metal ions with FAAS.

2.5. Adsorption kinetics studies

To study the adsorption kinetics of a metal ions, the modified Fe_3O_4 (0.025 g) was incubated with 5.0 mL of the solutions (at a specific pH), containing 50 mg L^{-1} of each metal ions, and the suspension was immediately stirred (150 rpm) for different periods of time. Adsorption kinetic data were obtained by measuring the concentration of metal ions in the solution at different times after removing the magnetic nanoparticles.

2.6. Characterization of Fe_3O_4 and ARS-Fe_3O_4

The peaks positions and relative intensities observed in XRD patterns of ARS-Fe_3O_4 nanoparticlesand standard Fe_3O_4 are shown in Fig. 1 for comparison. Five characteristics peaks for both Fe_3O_4 and ARS-Fe_3O_4 corresponding to indices (220), (311), (400), (511) and (440) were observed. Analysis of XRD patterns of Fe_3O_4 and ARS-Fe_3O_4 indicated very distinguishable peaks for magnetite crystal, which means that these particles have phase stability [25- 26].

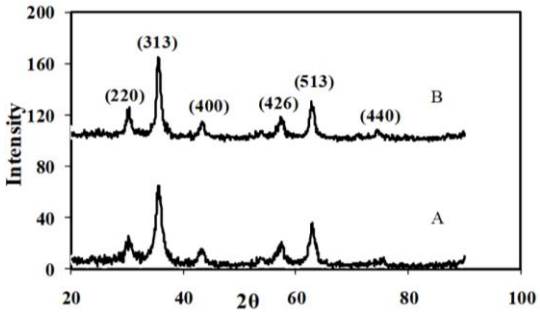

Fig. 1.XRD pattern of Fe_3O_4, A; and ARS-Fe_3O_4, B.

The FTIR spectra of Fe_3O_4, ARS and ARS-Fe_3O_4 are shown in Fig. 2A-2C. In the case of Fe_3O_4, the broad absorption band at 3200-3500 cm^{-1} indicates the presence of surface hydroxyl groups (O–H stretching). The bands at low wave numbers (700 cm^{-1}) are related to vibrations of Fe−O bonds of magnetite nanoparticles.

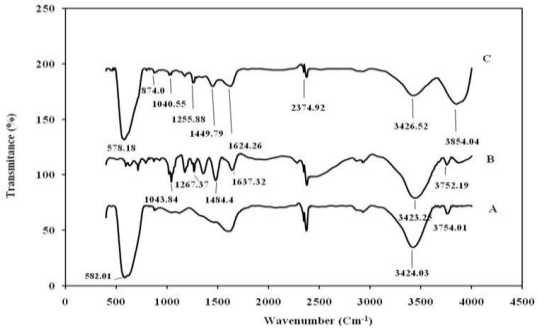

Fig. 2. FTIR spectra of Fe_3O_4, A; ARS, B; and ARS-Fe_3O_4, C.

The presence of magnetite nanoparticles can be verified by appearance of two strong absorption bands around 632 and 585 cm^{-1} [27- 28]. In the spectrum of ARS and ARS- Fe_3O_4 (Fig. 2A-2C), the broad peak at 3200–3500 is attributed to the stretching of bonded hydroxyl group. Theband around 2900 cm^{-1} shows C-H stretching of aromatic ring. C=O and C=C in ARS gives significantly stronger peaks in the ranges of 1400-1650 cm^{-1}. In the FTIR spectrum of ARS-Fe_3O_4, the significant absorption band at 2925 cm^{-1} is due to the C-H stretching. The absorption bands indicate to the SO_3 stretching and C-O stretchingin ARS-Fe_3O_4 around 1000-1300 cm^{-1} and the Fe-O bonds in magnetite nanoparticles shows at 578 cm^{-1}. After modifying, the peak shift from 578 to 582 cm^{-1} for Fe-O bond

vibration and similarly, a shifted in the peaks of S=O and O–H stretching towards lower or higher wavenumber, respectively, were observed indicating the developed interaction between Fe_3O_4 and ARS. The results showed that the functional groups of ARS might be involved in developing attraction forces between Fe_3O_4 nanoparticles and ARS through electrostatic interaction and hydrogen bonding. The modification with ARS at lower pH values was more significant probably due to the electrostatic attractions between negatively-charged ARS and positively-charged nanoparticles.

Fig. 3A is the representative TEM image of Fe_3O_4 and ARS-Fe_3O_4 nanoparticles. The average diameter of Fe_3O_4 nanoparticles was about ~10 nm. However, the TEM image (Fig. 3B) indicates that ARS-Fe_3O_4 (~15 nm) had a larger particle diameter than Fe_3O_4.

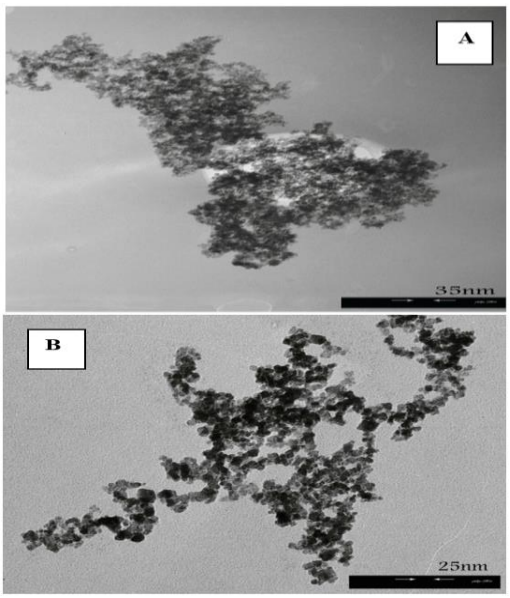

Fig. 3. The TEM image of Fe_3O_4, A and ARS- Fe_3O_4, B.

3. RESULT AND DISCUSSION

Some heavy metals (e.g., Cu^{2+} and Zn^{2+}) are essential for plant and animal health. However, at environmental concentrations above those necessary to sustain life, toxicity may occur. Other heavy metals (e.g Pb^{2+}) are not known to be essential to plants and animals and toxicity may occur when these metals become concentrated in the environment above the background levels [29]. So specificly, Zn^{2+}, Cu^{2+} and Pb^{2+} were studied. The efficiency of the prepared ARS-Fe_3O_4 as adsorbents for removal of Zn^{2+}, Cu^{2+} and Pb^{2+} from their individual aqueous solutions was investigated under different experimental conditions in order to find their optimum values as discussed below.

3.1. Effect of contact time

Contact time is an important factor in evaluating theadsorption efficiency, which helps to determine the rateof maximum removal of solutes. The effect of contact time on the performance of ARS-Fe_3O_4 nanoparticles for adsorption of three metal ions was investigated. AnARS-Fe_3O_4 amount of 0.025 g and a solution pH of 4.5 were considered for following this investigation. The initial metal ions concentration for all tested solutions were 50 mg L^{-1}. Fig. 4 shows removal efficiencies for three metal ions as a function of stirring time in the range of 2-25 minutes.

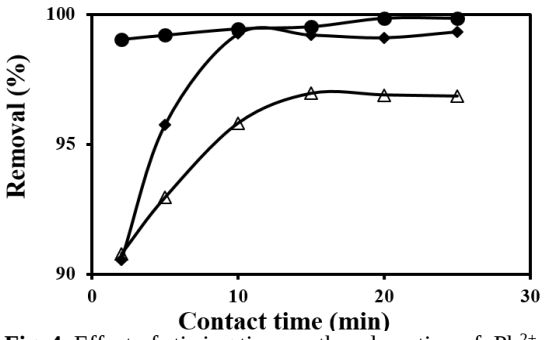

Fig. 4. Effect of stirring time on the adsorption of: Pb^{2+}, (●); Zn^{2+}, (♦); and Cu^{2+}, (Δ). Experimental conditions: ARS-Fe_3O_4 amount of 0.025 g, initial metal ion concentration of 50 mg L^{-1} at pH value 4.5.

The results indicate that the adsorption processes for three metal ions started immediately upon addition of ARS-Fe_3O_4. The removal efficiency for Cu^{2+} and Zn^{2+} rapidly increased from 90%, in the first minute of contact, to a value of 97% and 99%, respectively, after stirring time of 15 and 10 and where the equilibrium condition was attained. For Pb^{2+}, the percentage of removal, obtained in the first minute of stirring, was 99%; complete removal (99.8) was attained when the stirring was done for 5 minutes. Therefore, the optimum contact time between sample solution and ARS-Fe_3O_4 nanoparticles was considered to be 15, 10 and 5 minutes for Zn^{2+}, Cu^{2+} and Pb^{2+}, respectively. The rapid adsorption, at the initial contact time, is due to the availability of functional groups of ARS on surfaces of nanoparticles which led to a complexation between metal ions and dye. The presence of ARS onto the surface of nanoparticles increases interactions between ARS-Fe_3O_4 and metal ions. This also shortens the contact time required for metal ions to be quantitatively removed by ARS-Fe_3O_4.

3.2. Effect of ARS-Fe_3O_4 amount

The effect of ARS-Fe_3O_4amount on adsorption of Zn^{2+}, Cu^{2+} and Pb^{2+}, from their individual

solutions, was investigated using a batch technique by adding a known quantity of the adsorbent, in the range of 5-30 mg, into individual beakers containing 5 mL of the metal ions solution. The resulted suspensions were immediately stirred with a magnetic stirrer for 15, 10 and 5 minutes for Zn^{2+}, Cu^{2+} and Pb^{2+}, respectively. After the mixing time elapsed, the ARS-Fe_3O_4 nanoparticles were magnetically separated and the solutions were analyzed for the metal ions residue. For all measurements, the initial metal ions concentrations were fixed at 50 mg L^{-1} while the value of pH was 4.5. Results in Fig. 5 indicate that 82% of Cu^{2+}, 87% of Zn^{2+} and 98% of Pb^{2+} were removed from their individual aqueous solutions when an initial amount of 10 mg ARS-Fe_3O_4 was used. The percent removals of three metal ions increased with increasing ARS-Fe_3O_4(up to the amount of 10 mg) and eventually reached to the values of 99.2%,100.0% and 100 for Zn^{2+}, Cu^{2+} and Pb^{2+}, respectively. This observation can be explained by the fact that more adsorption sites would be available for metal ions at higher amount of ARS-Fe_3O_4.

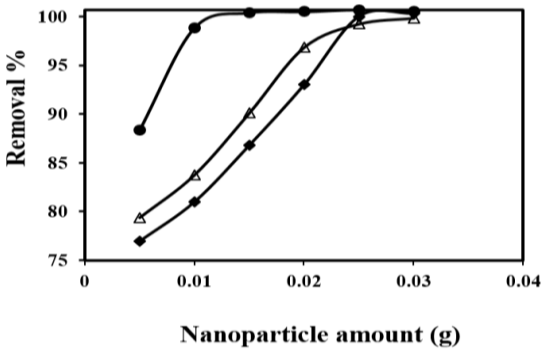

Fig. 5. Effect of nanoparticles amount on the adsorption of: Pb^{2+}, (●); Zn^{2+}, (♦); and Cu^{2+}, (Δ). Experimental conditions:, initial metal ion concentration of 50 mg L^{-1} at pH value 4.5, stirring time of (Pb^{2+}, 5; Zn^{2+}, 10 and Cu^{2+}, 15 minutes).

3.3. Effect of initial pH

The pH plays an important role in metal adsorption which is related to both the metal species and the availabilityof binding site which depends on the functional group of the sorbent [30]. The metal species, M(II); Cu(II), Pb(II) and Zn (II) are present in forms of M^{2+}, $M(OH)^{+}$, $M(OH)_2$(solid), etc. in water [30]. The solubility of the $M(OH)_2$(solid) is very high at pH ~5.0, so a large amount of the M^{2+} presents as main species. When pH is increasing the solubility of $M(OH)_2$(solid) decrease resulting in the main species in the solution is $M(OH)_2$(solid). It can be tell that the M^{2+} mustbe much more reduce at higher pH, but the major process for removing the M^{2+} is the precipitation, not adsorption [31].

The influence pH of solution on the extent of adsorption of magnetic nanoparticle shown in Fig. 6. The removal of Zn^{2+}, Cu^{2+} and Pb^{2+} from solution by adsorption is highly dependent on the pH of the solution. It was found that between 99.0% and 100% removal of the metal ionsachieved in pH between 5.0 and 6.0. At pH values higher than 6.0 insoluble metal hydroxide starts, precipitating from the solutions making true adsorption studies impossible. At pH <5.0, decrease in the removal efficiency could be due to the competition of hydronium ion toward complexation with alizarin red S. Therefore, the adsorption capacity was higher in pH range of 5.0-6.0 for all cases.

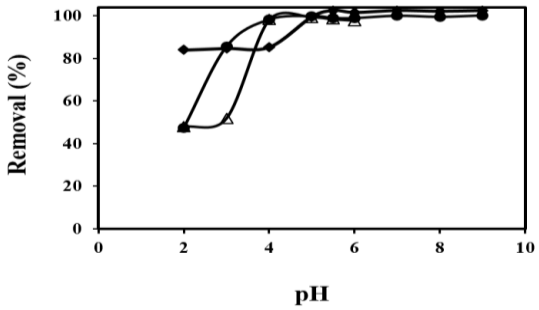

Fig. 6. Effect of pH of the sample solution on adsorption of Pb^{2+}, (●); Zn^{2+}, (♦); and Cu^{2+}, (Δ). Experimental conditions: ARS-Fe_3O_4 amount of 0.01 g, stirring time of (Pb^{2+}, 5; Zn^{2+}, 10; and Cu^{2+}, 15 minutes) initial metal ion concentration of 50 mg L^{-1}.

3.4. Effect of metal ions concentration.

The initial metal ions concentration is an important parameter that can affect its adsorption process. This will determine the concentration range of metal ions that could be quantitatively adsorbed, i.e. the concentration range for which the adsorption efficiency is high and independent of the initial concentration of metal ions. To obtain this, different concentrations of Zn^{2+}, Cu^{2+} and Pb^{2+} were studied for their removal by ARS-Fe_3O_4 under optimum experimental conditions. The results, in terms of removal efficiency versus initial concentrations of metal ions, are shown in Fig. 7.

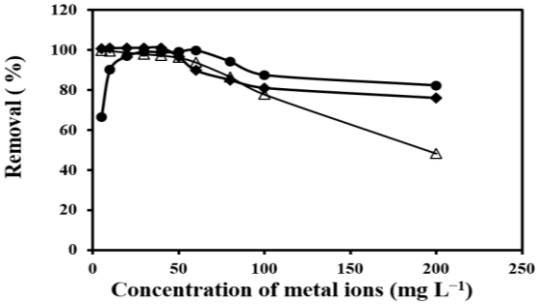

Fig. 7. Effect of initial metal ion concentration on adsorption of Pb^{2+}, (●); Zn^{2+}, (♦); and Cu^{2+}, (Δ). Experimental conditions: ARS-Fe_3O_4 amount of 0.01 g,

stirring time of (Pb^{2+}, 5; Zn^{2+}, 10; and Cu^{2+}, 15 minutes), pH value 5.0.

3.5. Effect of solution temperature

The effect of temperature on the adsorption of Zn^{2+}, Cu^{2+} and Pb^{2+} (50 mg L^{-1}) from their individual solutions on 0.025 g of ARS-Fe_3O_4 nanoparticles was studied at pH with a stirring time of 15, 10 and 5 minutes. A thermo shaker was used for adjusting of temperature and shaking. Fig. 8 shows the removal efficiencies for three metal ions as a function of temperature ranging between 298 and 328 K.

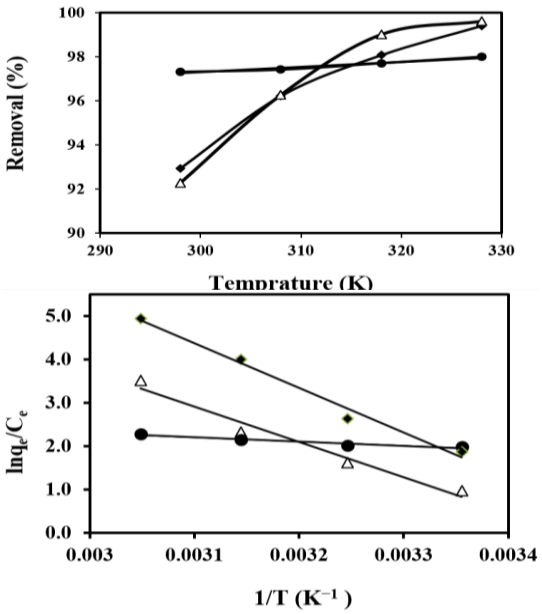

Fig. 8. (A) Effect of temperature on adsorption of: Pb^{2+}, (●); Zn^{2+}, (♦); and Cu^{2+}, (Δ). (B), the plots of $\ln(q_e/C_e)$ against 1/T for Pb^{2+}, (●); Zn^{2+}, (♦); and Cu^{2+}, (Δ). Experimental conditions:, ARS-Fe_3O_4 amount of 0.01 g, initial metal ion concentration of 50 mg L^{-1} at optimized pH value 5.0 and stirring time of (Pb^{2+}, 5; Zn^{2+}, 10; and Cu^{2+}, 15 minutes).

The results indicate that solution temperature strongly affected the adsorption efficiency of three metal ions. For instance, the adsorption efficiencies of both Cu^{2+} and Zn^{2+} were about 93% at 298 K and eventually reached to values of 99.4% and 100.8% at 328 K, respectively, indicating to an endothermic nature of the adsorption processes. The changes in standard free energy as well as changes in enthalpy and entropy of adsorption were calculated using van't Hoff equation:

$$\Delta G^0 = -RT\ lnK_c \qquad (1)$$

$$lnK_c = -\frac{\Delta H^0}{RT} + \frac{\Delta S^0}{R} \qquad (2)$$

Where ΔS° and ΔH° are change in entropy and enthalpy of adsorption, respectively. The Kc is the ratio of adsorbate concentration on adsorbent at equilibrium (q_e) to the remaining adsorbate concentration in the solution at equilibrium (C_e). The values of ΔH° and ΔS° were evaluated from the slope and intercept of van't Hoff plot (Table 1). The results indicate that the adsorption processes for three metalions are endothermic. The negative value of ΔG° indicates that the adsorption processes for three metal ions are spontaneous. The direct dependency of the negative value of ΔG° to temperature indicates that the spontaneity of adsorption is proportional to temperature. The positive value of ΔH indicates that adsorption processes for three metal ions onto ARS-Fe_3O_4 are endothermic. Thermodynamic studies revealed that greater adsorption can be obtained at higher temperatures. The values of entropy for adsorption of Zn^{2+}, Cu^{2+} and Pb^{2+} were 233.3, 295.5 and 40.2 J $mol^{-1}K^{-1}$, respectively. The positive value of ΔS° suggests randomness increasing at the solid/solution interface during the adsorption of three metal ions [32-33].

Table 1. Thermodynamic parameters of metal ions-adsorption process onto ARS-Fe_3O_4 nanoparticle.

Metal ion	ΔS_0^T (J mol^{-1} K^{-1})	ΔH_0^T (kJ mol^{-1})	ΔG_0^T (kJmol^{-1})			
			298 K	308 K	318 K	328 K
Cu^{2+}	233.3	67.45	−2.68	−4.40	−6.73	−9.07
Zn^{2+}	295.48	83.60	−4.45	−7.4	−10.36	−13.32
Pb^{2+}	40.18	7.09	−4.9	−5.3	−5.7	−6.09

3.6. Adsorption isotherm modeling

Several isotherm models for evaluating the equilibrium adsorption, has discussed in literatures [34]. For evaluating the equilibrium adsorption, Langmuirand Freundlichisotherm models were used. The linearized form of the Langmuir isotherm, assuming monolayer adsorption on a homogeneous adsorbent surface, is expressed as:

$$\frac{C_e}{q_e} = \frac{1}{bq_{max}} + \frac{C_e}{q_{max}} \qquad (3)$$

whereq_{max} (mg g^{-1}) is the surface concentration at monolayer coverage and illustrates the maximum value of q_e that can be attained as C_e is increased. The b parameter is a coefficient related to the

energy of adsorption and increases with increasing strength of the adsorption bond. Values of q_{max} and b are determined from the linear regression plot of (C_e/q_e) versus C_e.

The Freundlich equation is expressed in its linear form as follows:

$$logq_e = logK_F + \frac{1}{n} logC_e \qquad (4)$$

where K_F and n are the constants from the Freundlich equation representing the capacity of the adsorbent for the adsorbate and the reaction order, respectively. The reciprocal reaction order, 1/n, is a function of the strength of adsorption.

The equilibrium adsorption data for Zn^{2+}, Cu^{2+} and Pb^{2+} were analyzed using Langmuir and Freundlich, models. Models fitted to equilibrium adsorption results of three metal ions were assessed based on the values of the correlation coefficients (R^2) of their linear regression plots. The experimental data fitted with two models indicated that the adsorptions of Zn^{2+}, $Cu^{2+}$and Pb^{2+} on ARS-Fe_3O_4 nanoparticles are better described by the Langmuir model. The resulting plots for Langmuir model are shown in Table 2 summarize the model constants and the correlation coefficient.

Table 2. Adsorption isotherm parameters for adsorption of Cu^{2+}, Zn^{2+} and Pb^{2+} onto ARS-Fe_3O_4 nanoparticle.

	Langmuir model			Freundlich model		
Metal ion	q_{max} (mg g^{-1})	b	R^2	K_F(mg g^{-1})	n (g L^{-1})	R^2
Cu2+	22.7	0.33	0.986	57.4	1.8	0.935
Zn2+	50.0	1.33	0.989	2.04	1.42	0.840
Pb2+	21.7	1.0	0.989	11.0	1.66	0.913

Three metal ions were adsorbed on ARS-Fe_3O_4 nanoparticlesdue to itscomplexation with Alizarin red S. The maximum adsorption capacity of ARS-Fe_3O_4 nanoparticle for Zn^{2+}, Cu^{2+} and Pb^{2+} is 50.0, 22.7 and 21.7 mg of metal ions per gram of nanoparticle.

Table 3 presents a comparison between the adsorption capacity (obtained based on the Langmuir model) of the developed adsorbent and another adsorbent reported in literature for adsorption of Zn^{2+}, Cu^{2+} and Pb^{2+} [29, 35,36].

Table 3. Comparisons of the proposed adsorbent and other adsorbent for the adsorption of Pb^{2+}, Zn^{2+} and Cu^{2+}.

Adsorbent	Metal ions	q_m (mgg^{-})	K_L (L g^{-1})	Reference
Rice Husk	Pb^{2+}	0.651	186.67	[35]
	Zn^{2+}	19.74	0.066	
Aminated Polyacrylo-nitrile Nanofiber Mats	Pb^{2+}	15.75	22.90	[36]
	Cu^{2+}	30.40	23.70	
Kaolinite	Pb^{2+}	7.75	0.003	[29]
	Zn^{2+}	4.95	0.001	
	Cu^{2+}	4.42	0.001	
ARS-Fe_3O_4	Pb^{2+}	21.7	1.00	This work
	Zn^{2+}	50.0	1.33	
	Cu^{2+}	22.7	0.33	

3.7. Adsorption kinetic modeling

Several models are available to study the adsorption mechanism and describe the corresponding experimental data. The most commonly models used are the pseudo-first-order and pseudo-second-order reaction rate equations developed by Ho and McKay [37].

Pseudo-first-order equation:

$$\log(q_e - q_t) = \log q_e - k_1^t \qquad (5)$$

Pseudo-second-order equation:

$$\frac{t}{q_t} = \frac{1}{k_2 q_e^2} + \frac{t}{q_e} \qquad (6)$$

where k_1 and k_2 are the adsorption rate constants, q_t is adsorption capacity at time t, q_e is adsorption capacity at equilibrium condition.

To describe the adsorption behavior and rate, the data obtained from adsorption kinetic experiments were evaluated using pseudo-first-order and pseudo-second-order reaction rate models. Experimental results of the three metal ions fitted to the selected adsorption model are shown in Table 4.

Table 4 gives a summary of the models and the corresponding constants along with the correlation coefficients for the linear regression plots of the three tested metal ions. Higher values of R^2 were obtained for pseudo-second order than for pseudo-first order adsorption rate models indicating that the adsorption rates of Zn^{2+}, Cu^{2+} and Pb^{2+} onto ARS-Fe_3O_4 nanoparticles can be more appropriately described using the pseudo-second-order rate [37].

Table 4. Adsorption kinetic constants for Cu^{2+}, Zn^{2+} and Pb^{2+} ontoARS-Fe_3O_4 nanoparticles.

	Pseudo-first-order model			Pseudo-second-order model			Intra-particle diffusion		
Metal ion	k_1 (min^{-1})	q_e (mgg^{-1})	R^2	k_2 ($gmg^{-1}min^{-1}$)	q_e ($mg\ g^{-1}$)	R^2	k_i ($g\ mg^{-1}min^{-1}$)	C ($mg\ g^{-1}$)	R^2
Cu^{2+}	0.22	1.1	0.982	0.47	9.80	1.00	0.288	8.66	0.998
Zn^{2+}	0.02	137	0.996	0.90	8.33	0.999	0.412	6.99	0.978
Pb^{2+}	0.07	0.5	0.978	1.1	29.4	1.00	0.066	28.69	0.993

Intra-particle diffusion is a transport process involving movement of species from the bulk of the solution to the solid phase. The intra-particle kinetic model is expressed by:

$$Q_t = k_i t^{1/2} + C \qquad (7)$$

Wherek_i is an intra-particle diffusion rate constant and Q_t is amount of adsorbate adsorbed at time t. Initially, the external surface adsorption, which is faster, is completed and then, the intra-particle diffusion is attained. A plot of the amount of analyte adsorbed, q_t ($mg\ g^{-1}$) vs. the square root of the time, gives the rate constant (slope of the plot) and the intercept is proportional to the boundary layer thickness.

Intra-particle diffusion [38] is a transport process involving movement of species from the bulk of the solution to the solid phase surface. The mechanism for adsorption of a metal ions on nanoparticles is assumed as a three-step process in which bulk diffusion, i.e. migration of the metal ions from the bulk of the solution to the boundary layer nearby the surface of the nanoparticle, is not considered. The first step is diffusion of metal ions through the boundary layer toward the surface of the adsorbent. The second step is the metal ions transfer from the exterior surface of the adsorbent particle to the interior pores of the particle through a pore diffusion or intra-particle diffusion mechanism. Finally, the adsorption occurs onto an active site of adsorbent via an ion exchange and/or a complexation process [39-41]. According to intra-particle diffusion model, the plot of uptake should be linear if intraparticle diffusion is involved in an adsorption process. If this line passes through the origin then intra-particle diffusion is the rate-controlling step. When the plot does not pass through the origin, this is indicative of some degree of boundary layer control. This shows that the intra-particle diffusion is not the only rate limiting step, but also other kinetic models may control the rate of adsorption, all of which may be operating simultaneously [38]. According to the intra-particle diffusion model, the slope of the linearized plot characterizes the rate parameter of the diffusion, whereas the intercept is proportional to the boundary layer thickness. In this study, the correlation coefficient (R^2) value of the model indicates the possibility of intra-particle diffusion (Table 4) for the metal ions adsorbed onto magnetic nanoparticles.

3.8. Desorption and reusability studies

In this regard, the reusability of the nanoparticles was an important factor to be studied. Possible desorption of Zn^{2+}, Cu^{2+} and Pb^{2+} were tested by EDTA (0.01, 0.1 mol L^{-1}) and HCl (0.01, 0.1 mol L^{-1}) solutions. The desorption ratio was calculated as the ratio of the amount of metal ions in the desorption medium to the amount of metal ions initially adsorbed on ARS-Fe_3O_4 nanoparticles. The results showed that the desorption ratios were about 101%, 94% and 102% (in HCl at 0.1 mol L^{-1}) for Zn^{2+}, Cu^{2+} and Pb^{2+}, respectively. The study revealed that the adsorbed Zn^{2+}, Cu^{2+} and Pb^{2+} could be completely desorbed in the presence of HCl. In this study more than 94-102% of metal ions could be desorbed and recovered by 2 mL of HCl (0.1mol L^{-1}) in 15 minutes, when 50 µg ofmetalionswas already adsorbed on 25.0 mg [ARS]-Fe_3O_4 nanoparticles.

The reusability of the adsorbents in several successive separation processes was tested and the result showed that the [ARS]-Fe_3O_4 nanoparticles can be reused for three times without significant reduction in its removal capacity. After being used for three times, the adsorption efficiencieswere reduced to about 5.5, 10.4 and 15.3 %, respectively, for Zn^{2+}, Cu^{2+} and Pb^{2+}. Considering the reproducibility of the results (RSD), these data indicated that the adsorbent was better not to be used more than 3 times.

4. CONCLUSIONS

The ARS-Fe_3O_4 nanoparticles were quite efficient as magnetic nano-adsorbents for fast adsorption of metal ions from aqueous solutions. The time required to achieve the adsorption equilibrium was 15, 10 and 5 minutes for Zn^{2+}, Cu^{2+} and Pb^{2+},

respectively. The adsorption of the tested metal ions on the surface of ARS-Fe_3O_4 nanoparticles was concluded due to itscomplexation with Alizarin red S.The experimental data fitted with Langmuir and Freundlichmodels indicated that the adsorptions of Zn^{2+}, Cu^{2+} and Pb^{2+} on ARS-Fe_3O_4 nanoparticles are better described by the Langmuir model. The changes of enthalpy (ΔH) were determined to be 67.45 and 83.60 and7.09 kJ mol^{-1} for Zn^{2+}, Cu^{2+} and Pb^{2+} in the same order. Kinetic data were appropriately fitted to the pseudo-second order adsorption rates. The HCl (0.1 mol L^{-1})solution was suitable for desorption of Zn^{2+}, Cu^{2+} and Pb^{2+}; the reusability of ARS-Fe_3O_4 was found to be for three times. It would be better to study the adsorption of these three metal ions simultaneously, this suggestion will be considered as a future study .

Considering the objective of the work that could be deduced from the title of the paper, a comparative study between Fe_3O_4 and ARS-Fe_3O_4 has not been performed. However, the results could be used for being compared with other dyes that have been used for modification of Fe_3O_4 nanoparticles [42].

ACKNOWLEDGMENTS

The authors wish to acknowledge the support of this work by Payame Noor University. We would like to thank E. Seyghalani Talab of Payame Noor University, Prof. G. Absalan of Department of Chemistry, Department of Physics, Department of Engineering and Veterinary College at Shiraz University for their technical assistance.

REFERENCES

[1] J. Song, H. Kong, J. Jang, Adsorption of heavy metal ions from aqueous solution by polyrhodanine-encapsulated magnetic nanoparticles, *J. Colloid Interface Sci.* 359 (2011) 505–511.

[2] M.A.Tofighy and T. Mohammadi, Adsorption of divalent heavy metal ions from water using carbon nanotube sheets, *J. Hazard. Mater.* 185 (2011) 140–147.

[3] G. Rao, C. Lu and F. Su, Sorption of divalent metal ions from aqueous solution bycarbon nanotubes: a review, *Sep. Purif. Technol*. 58 (2007) 224–231.

[4] Y.H. Li, J. Ding, Z. Luan, Z. Di, Y. Zhu, C. Xu, D. Wu and B. Wei, Competitive adsorption of Pb^{2+}, Cu^{2+} and Cd^{2+} ions from aqueoussolutions by multiwalled carbon nanotubes, *Carbon* 41 (2003) 2787–2792.

[5] M.M. Rao, A. Ramesh, G.P.C. Rao, K. Seshaiah, Removal of copper and cadmiumfrom the aqueous solutions by activated carbon derived from ceibapentandrahills, *J. Hazard. Mater. B* 129 (2006) 123–129.

[6] M. Secar, V. Sakthi and S. Rengaraj, Kinetics equilibrium adsorption study of lead(II)onto activated carbon from coconut sell, *J. Colloid Interface Sci.* 279 (2004) 307-313.

[7] J. Ayala, F. Blanco, P. Garcia, P. Rodriguez and J. Sancho, Asturian fly ash as a heavymetals removal material, *Fuel.* 77 (1998) 1147–1154.

[8] C.H. Weng and C.P. Huang, Adsorption characteristics of Zn(II) from dilute aqueoussolution by fly ash, *Colloid. Surf. A* 247 (2004) 137–143.

[9] Y.S. Ho and G. McKay, The sorption of lead (II) ions on peat, *Water Res.* 33 (1999)584-578.

[10] S.C. Pan, C.C. Lin and D. Hwa, Reusing sewage sludge ash as adsorbent forcopper removal from waste water, *Resour. Conserv. Recy.* 39 (2003) 79-80.

[11] B. Biscup and B. Subotic, Removal of heavy metal ions from solutions using zeolites.III. Influence of sodium ion concentration in the liquid phase on the kinetics ofexchange processes between cadmium ions from solution and sodium ionsfromzeolit A, *Sep. Sci. Technol.* 39 (2004) 925–940.

[12] Q. Li, S. Wu, G. Liu, X. Liao, X. Deng, D. Sun, Y. Hu and Y. Huang, Simultaneous-biosorption of cadmium (II) and lead (II) ions by pretreated biomass of phanerochaete-chrysosporium, *Sep. Purif. Technol. 34* (2004) 925–940.

[13] F. Ekmekyapar, A. Aslan, Y.K. Bayhan and A. Cakici, Biosorption of copper(II) byNonliving lichen biomass of cladoniarangoformishoffm, *J. Hazard. Mater.* 137 (2006) 293-298.

[14] W. Chu, Lead metal removal by recycled alum sludge, *Water Res.* 33 (1999) 2025-3019.

[15] R. Sublet, M.O. Simonnot, A. Boireau and M. Sardin, Selection of an adsorbent forlead removal from drinking water by a point-of-use treatment device, *WaterRes.* 37 (2003) 4904–4912.

[16] P. Brown, I.A. Jefcoat, D. Parrish, S. Gill and S. Graham, Evaluation of the adsorptivecapacity of peanut hull pellets for heavy metals in solution, *Adv. Environ. Res.* 4 (2000) 19-29.

[17] M. Arias, M.T. Barral and J.C. Mejuto, Enhancement of copper and cadmium adsorptionon kaolin by the presence of humid acids, *Chemosphere* 48 (2002) 1081-1088.

[18] C.V. Diniz, F.M. Doyle and V.S.T. Ciminelli, Effect of pH on the adsorption of

selectedheavy metal ions from concentrated chloride solutions by the chelating resindowex M-4195, *Sep. Sci. Technol.* 37 (2002) 3169–3185.

[19] M. Hossein, N. Dalali, A. Karimi, K. Dastanra, Solid phase extraction of copper, nickel and cobalt in water samples using surfactant coated alumina modified with indane-1,2,3-trione 1,2-dioxime and determination by flame atomic absorption spectrometry, *Turk. J. Chem.* 34 (2010) 805 – 814.

[20] M. Hossein, N.Dalali, S. Mohammad nejad, Preconcentration of trace amounts of copper(II) on octadecyl silica membrane disks modified with indane-1,2,3-trione 1,2-dioxime prior to its determination by flame atomic absorption spectrometry, *Int. J. Ind. Chem*. 3 (2012) 7.

[21] P. Wang, M. Du, H. Zhu, S. Bao, T. Yang and M. Zou, Structure regulation of silica nanotubes and their adsorptionbehaviors for heavy metal ions: pH effect, kinetics,isotherms and mechanism, *J. Hazard. Mater.* 286 (2015) 533–544.

[22] X. Yu, S. Tong, M. Ge, L. Wu, J. Zuo, C. Cao and W. Song, Adsorption of heavy metal ions from aqueous solution by carboxylatedcellulosenanocrystals, *J. Environ. Sci. 25* (2013) 933–943.

[23] L. Bromberg, S. Raduyk and T. A. Hatton, Functional magnetic nanoparticles for biodefense and biological threat monitoring and surveillance, *Anal. Chem.* 81 (2009) 5637–5645.

[24] D.K. Kim, Y. Zhang, W. Voit, K.V. Rao, M. Muhammed, Synthesis and characterization of surfactant-coated superparamagnetic-monodispersed iron oxide nanoparticles, *J. Magn. Magn. Mater.* 225 (2001) 30-36.

[25] S.I. Park, J.H. Kim, J.H. Lim and C.O. Kim, Surface-modified magnetic nanoparticles with lecithin for applications in biomedicine, *Curr. Appl. Phys.* 8 (2008) 706–709.

[26] D. Faivre and P. Zuddas, An integrated approach for determining the origin of magnetite nanoparticles, *Earth Planet Sci. Lett.* 243 (2006) 53-60.

[27] R.D. Waldron, Infrared spectra of ferrites, *Phys. Rev.* 99 (1955) 1727-1735.

[28] K. Can, M. Ozmen and M. Ersoz, Immobilization of albumin on aminosilane modified superparamagnetic magnetite nanoparticles and its characterization, *Colloids Surf. B Biointerfaces* 71 (2009) 154-159.

[29] S. Shahmohammadi-Kalalagh, H. Babazadeh, A. H. Nazemi and M. Manshouri, Isotherm and Kinetic Studies on Adsorption of Pb, Zn and Cu by Kaolinite, *Caspian J. Env. Sci.* 9 (2011) 243-255.

[30] A. Afkhami, M. Saber-Tehrani and H. Bagheri, Simultaneous removal of heavy-metal ions in wastewater samples using nano-alumina modifiedwith 2,4-dinitrophenyl-hydrazine, *J. Hazard. Mater.* 181 (2010) 836–844.

[31] V.C. Srivastava, I.D. Mall and I.M. Mishra, Removal of cadmium(II) and zinc(II) metal ions from binary aqueous solution by rice husk ash, *Colloid. Surf. A* 312 (2008) 172–184.

[32] Z. Zhang, I.m. O'Hara, G.A. Kent and W.O.S. Doherty, Comparative study on adsorption of two cationic dyes by milled sugarcane Bagasse, *Ind. Crop. Prod.* 42 (2013) 41-49.

[33] M. Ghaemi and G. Absalan, Study on the adsorption of DNA on Fe_3O_4 nanoparticles and on ionic liquid-modified Fe_3O_4 nanoparticles, *Microchim. Acta* 181 (2014) 45-53.

[34] G. Limousin, P. Gaudet, L. Charlet, S. Szenknect, V. Barthés and M. Krimissa, Sorption isotherms: A review on physical bases, modeling and measurement, *Appl. Geochem.* 22 *(*2007) 249-275.

[35] E. Asrari, H. Tavallali and M. Hagshenas, Removal of Zn(II) and Pb (II) ions Using Rice Husk in Food Industrial Wastewater, *J. Appl. Sci. Environ. Manage.* 14 (2010) 159 – 162.

[36] P. Kampalanonwat and P. Supaphol , The Study of Competitive Adsorption of Heavy Metal Ions from Aqueous Solution by Aminated Polyacrylonitrile Nanofiber Mats, *Energy Procedia*. 56 (2014) 142–151.

[37] Y.S. Ho and G. McKay, Pseudo-second-order model for sorption processes, *Process Biochem.* 34 (1999) 45-465 .

[38] B. Saha, S. Das, J. Saikia and G. Das, Preferential and Enhanced Adsorption of Different Dyes on Iron Oxide Nanoparticles: A Comparative Study, *J. Phys. Chem. C* 115 (2011) 8024-8033.

[39] Y. Yang, D. Jin, G. Wang, D. Liu, X. Jia and Y. Zhao, Biosorption of Acid Blue 25 by unmodified and CPC-modified biomass of Penicillium YW01: Kinetic study, equilibrium isotherm and FTIR analysis, *Colloids Surf. B* 88 (2011) 521-526 .

[40] K.A.G. Gusmaoa, L.V.A. Gurgel, T.M.S. Meloa and L.F. Gil, Application of succinylated sugarcane bagasse as adsorbent to remove methylene blue and gentian violet from aqueous solutions-Kinetic and

equilibrium studies, *Dyes Pigm.* 92 (2012) 967-974.

[41] K.Elass, A. Laachach, A. Alaoui and M. Azzi M, Removal of methyl violet from aqueous solution using a stevensite-rich clay from Morocco, *Appl. Clay Sci.* 54 (2011) 90-96.

[42] P. Yan, M. He, B. Chen and B. Hu, Restricted accessed nanoparticles for direct magnetic solid phase extraction of trace metal ions from human fluids followed by inductively coupled plasma mass spectrometry detection, *Analyst* 140 (2015) 4298-306.